

RESEARCH ARTICLE

CuO-NiO Nano composites: Synthesis, Characterization, and Cytotoxicity evaluation

Abbas Rahdar^{1*}; Mousa Aliahmad^{2*}; Yahya Azizi², Naser Keikha³, Mahdiyeh Moudi³, Farshid keshavarzi⁴

¹Departments of Physics, Faculty of Science, University of Zabol, Zabol, Iran

²Department of Physics, Faculty of Science, University of Sistan and Baluchestan, Zahedan, Iran

³Infectious Disease and Tropical Medicine Research Center, Zahedan University of Medical Sciences, Zahedan, Iran

⁴Department of Clinical Biochemistry, School of Medicine, Zahedan University of Medical Sciences, Zahedan, Iran

ARTICLE INFO

Article History:

Received 23 November 2016

Accepted 19 December 2016

Published 24 December 2016

Keywords:

Nano-composites

Cytotoxicity

Antifungal

ABSTRACT

Objective(s): In this work, CuO- NiO nano-composites were synthesized via free-surfactant co-precipitation method and then their physiochemical properties, as well as cytotoxicity and antifungal effects, were studied.

Methods: The structural and optical properties of CuO-NiO nanostructures were analyzed by X-ray diffraction (XRD), scanning electron microscopy (SEM), Atomic force microscope (AFM), UV-Vis absorption, and vibrating sample magnetometer (VSM) techniques. MTT assay was used to evaluate the cytotoxicity of nanostructures.

Results: The cubical structure of CuO- NiO nano-composites was confirmed by the XRD technique. The optical study of the samples by UV-Vis indicted a blue shift in absorption wavelength with decreasing particle size due to quantum size effect. The super magnetic behavior of CuO-NiO nano composites after calcination was confirmed by magnetic characterization instrument. Finally, the results of cytotoxicity evaluation of CuO-NiO nano-composites at the lower concentrations on Breast cancer MDA cell lines demonstrate no significant toxicity. Minimum inhibitory concentration range and Minimum fungicidal concentration of nanoparticle were determined 0.97-15.62, 7.81µg/ml and for fluconazole were 1.75-25 µg/ml and 12.58 µg/ml, respectively.

Conclusions: The study result of antimicrobial of CuO-NiO nano composites indicated an MIC90 antifungal activity with a concentration of 3.90µg/ml against vaginal isolates of *C. albicans*. The results of cytotoxicity study of nano-composites at concentration of 50µg/ml and 10µg/ml on the cell line of Breast cancer MDA was equivalent to %60 and %80, respectively.

How to cite this article

Rahdar A, Aliahmad M, Azizi Y, Keikha N, Moudi M, keshavarzi F, CuO-NiO Nano composites: Synthesis, Characterization, and Cytotoxicity evaluation. *Nanomed Res J*, 2017; 2(2):78-86. DOI: 10.22034/nmrj.2017.56956.1057

INTRODUCTION

The crystalline nanometer-sized particles have attracted a wide attention due to not only their major applications in the different scientific fields but also their biological applications to improve the environment and human health [1]. Nickel Oxide

* Corresponding Author Email: a.rahdar@uoz.ac.ir
aliahmad@phys.usb.ac.ir

(NiO) and Copper oxide (CuO) with an optical band gap of 3.6-4eV ($E_g=3.6-4$ eV) and 1.2eV ($E_g=1.2$ eV), respectively, act as a P-type semiconductor with application in a wide range of technologies such as sensors, optical devices, electrochemical super capacitor, as a transparent P-type semiconducting

layer and as an antiferromagnetic film and so on due to is the optical and magnetical unique properties [1-5].

The conducted researches state that the technological application of semiconductor materials can be enhanced via mixing and decreasing their dimensions in nanometer-sized scale [1-5]. Moreover, it must be pointed out that applied methods to synthesis nano-particles have a marked effect on the particle size. To this end, many methods have been developed to prepare nickel oxide nonmaterial, including low-pressure spray pyrolysis, surfactant-mediated method, simple liquid phase process, electro spinning, etc [10–17]. On the other hand, reported studies in the field of study of CuO-NiO nano composites have only been focused on their optical and magnetically properties [8-9], but not their biological study including the cytotoxicity and antifungal effects, to our knowledge.

It is important to mention that metal oxides nanostructures such as CuO–NiO nanocomposites. Due to their unique magnetical, optical, and molecular properties as a consequence of mixing the metal oxides of Nickel Oxide (NiO) and Copper oxide (CuO) [1-5] can be used in different biomedical fields such as nano-biosensor for clinical and non-clinical diagnostic applications [6-7], drug delivery, immunoassays, etc.

In a study conducted by Mahmoodi et al, CuO–NiO nanocomposites were suggested as an inorganic adsorbent to remove dye from water [36]. In addition, Devadathan and Raveendran studied the antifungal properties of metal oxide nanocomposites of nickel-zinc, and they reported an antifungal property of the nanocomposites for the fungi *Penicillium Chrysogenum* [37].

In another study, fabricated-bioactive glasses based on nanocomposites containing different CuO contents were introduced to inhibit infections resulting from implants [38]. With this in mind, in the current study, the CuO- NiO nanoscale-sized composites were synthesized via co-precipitation method in the absence of capping agent to avoid their toxic effect on biological systems, and changing copper percent in the solution, and then samples were characterized by the scanning electron microscopy (SEM), and X-ray diffraction (XRD) vibrating sample magnetometer (VSM), Energy-dispersive X-ray spectroscopy (EDS, EDX, or

XEDS), and atomic force microscopy (AFM) techniques, and then the cytotoxicity and antifungal effects of CuO- NiO nano composites on MDA cell line of Breast cancer and against vaginal isolates of *Candida albicans* were also studied as part of the study. In addition, it is of interest to note that *C. albicans* is an important human fungal pathogen. Although this opportunistic pathogen is a natural component of the human flora, it can cause life-threatening infections in immune-suppressed patients, Due to the multiple pathogenic factors. On the other hand Due to the increasing drug resistance of fungal infections caused by *Candida albicans* discovery of new antifungal drugs are necessary and essential.

MATERIALS AND METHODS

Reagents

NiCl₂·6H₂O, CuCl₂·2H₂O and NaOH (99.9 %, Merck Co.) were analytical grade , Breast cancer MDA cells (Pasteur Institute (Iran), Fluconazole (Amin pharmaceutical company, Iran), CHROMagar *Candida* medium (Paris, France), and Corn meal agar (Difco, USA) used as received without further purification and deionized water as solvent were used.

Synthesis of CuO-NiO Nano composites

To prepare CuO-NiO Nano composites via co-precipitation method without the surfactant, initially, a weight amount of 5.9412g of NiCl₂·6H₂O and 3.3409g of CuCl₂·6H₂O were separately dissolved in 50 mL of deionized water under stirring (A sample containing high Cu content), a weight amount of 5.9412g of NiCl₂·6H₂O and 4.2331g of CuCl₂·6H₂O were separately dissolved in 50 mL of deionized water under stirring (B sample containing low Cu content) at room temperature [4,8-9]. Then, intermixed solution containing a precursor of Nickel and Copper was magnetically stirred for 50min at 50°C temperature. Afterward, the 10cc NaOH (1M) was added drop by drop to the solution with constant Stirring until the pH becomes 8.

In the final step, the obtained green gel washed with deionized water to remove formed byproducts during the reaction process and dried at 60°C temperature for 14 hr. Then, dried samples were annealed at 500°C temperature for 2h to obtain CuO-NiO Nano composites. The color of samples

changed from green to black due to calcination process.

Characterization

X-ray diffraction pattern of nanoscale-sized structures was carried out by a diffract meter (Rigaku-Miniflex model equipped with a source of X-ray was $\text{CuK}\alpha$ and a wavelength of 1.5406 Å). Magnetization measurement of samples was performed by a vibrating sample magnetometer (VSM) tool (MDKFT, Kashan, Iran). The scanning electron microscopy (Philips XL10 model voltage 17kV) was used to study the morphology of particles. The elemental analysis of nano-composites was done by The EDAX tool (Philips XL10 model and the working voltage was 17 kV). Zetasizer Nano (Malvern Instruments, Germany) equipped with a He-Ne laser source (633nm) with vertically polarized light was used to calculate the hydrodynamic diameter of nanoparticles. The UV/Vis absorption spectrum of nanostructures was carried out by using a UV-1650 PC spectrometer (Shimadzu) in the wavelength of 200 to 700 nm.

Sample preparation

In this experimental study, we used of 41 clinical vaginal isolates of *Candida albicans* that were isolated from patients with vulvovaginal candidacies. All isolates were identified by germ tube production test, culture on CHROMagar *Candida* medium (Paris, France), and Cornmeal agar with 1% of tween 80 (Difco, USA). The determination of the minimum inhibitory concentration (MIC) was performed in 96-well plates using serial dilutions of a stock of sonicating (The Model 3000MP Ultrasonic Homogenizer) nano-composites according to the Clinical and Laboratory Standards Institute (NCCLS) M37-A3 document [30]. Fluconazole (Amin pharmaceutical company, Iran) was obtained for the preparation of the broth micro-dilution based on CLSI recommendations.

Cell viability assay

MDA cells were exposed to CuO-NiO nano-composites (10–50 µg/ml) for 24 h to evaluate their cytotoxicity by MTT assays. MDA cells of Breast cancer were cultured in the usual fashion as monolayers in RPMI1640 media enriched with 10% fetal bovine serum. The MDA cells (1×10^4

cells/well) were moved onto 96-well plates and at 24h post-seeding, different concentrations (i.e. ranging from 10 to 50 µg/ml) of nanometer-sized particles were added to each well. The treated cells were then incubated for 24h. After the defined time, cells were treated with (3-(4,5-dimethylthiazol-2-yl)-2,5-diphenyltetrazolium)bromide (MTT) [27-28]. The plates were then incubated for 3.5h at 37°C in a CO₂ incubator. Eventually, after removing the medium absorbance of the formed formazan crystals was read by adding 200 µl DMSO. Then the absorbance was evaluated at a wavelength of 570 nm using a spectrophotometer (Elisa reader, Biochrom Anthos 2020 microplate reader) and cell viability was studied according to the standard protocol [29].

In vitro antifungal assay

The determination of the minimum inhibitory concentration (MIC) was performed in 96-well plates (The Model 3000MP Ultrasonic Homogenizer) nano-composites according to the Clinical and Laboratory Standards Institute (NCCLS) M37-A3 document [30]. In this study, we used of 41 clinical vaginal isolates of *Candida albicans* that were isolated from patients with vulvovaginal candidacies. All isolates were identified by germ tube production test, culture on CHROMagar *Candida* medium (Paris, France), and Corn meal agar with 1% of tween 80 (Difco, USA). Fluconazole (Amin pharmaceutical company, Iran) was obtained for preparation of the broth micro-dilution based on CLSI recommendations.

RESULTS AND DISCUSSION

As stated in the Introduction, this research is aimed to understand physiochemical properties as well as cytotoxicity and antifungal effects of CuO-NiO nano-composites. In order to do this, the synthesized nano composites were characterized by different techniques including the scanning electron microscopy (SEM), X-ray diffraction (XRD) vibrating sample magnetometer (VSM), Energy-dispersive X-ray spectroscopy (EDS, EDX, or XEDS), and atomic force microscopy (AFM), and in final step, the cytotoxicity and antifungal effects of CuO- NiO nano composites on MDA cell line of Breast cancer and against vaginal isolates of *Candida albicans* were also studied as part of the study. Considering the above objectives, Fig. 1, shows

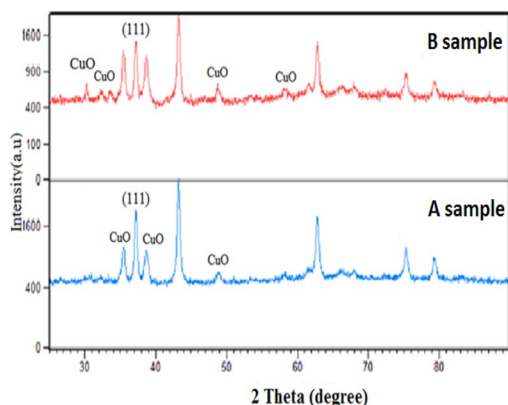


Fig. 1. XRD patterns of CuO-NiO Nanocomposites after calcinations

X-ray diffraction (XRD) pattern of the CuO-NiO Nano composites prepared via Co-Precipitation route at room temperature.

As seen in Fig.1, the Bragg peaks were obtained at 2Theta values of 37.1775, 43.1897, 62.7810, 75.2675, 79.2376 degrees correspond to planes of (111), (200), (220), (311) and (222) related to cubic structure of NiO and other 2Theta values of 35.5651, 38.6481, 48.8422 related to monoclinic structure of CuO for A sample (nano-composite containing low Cu content), that these results were matched with the observed values in JCPDS files (No.01-078-0648 and No. 00-049-1830, respectively).

As seen in Fig.1, the number of planes related to CuO increases with increase in Cu content in the nano-composite (B sample containing high Cu content). In addition, it observed that the peak intensity related to Ni decreases and the peak intensity of Cu increase as Cu content increases in the system.

It is clear from Fig. 1 that no other characteristic peak due to any impurities and sharp peaks are present in the pattern, indicating that the prepared samples are of high purity and crystallinity. The average crystallite size of 39, 34 nm were obtained for Nano composites A and B, respectively, using the Scherer's equation [18-20] by (111)

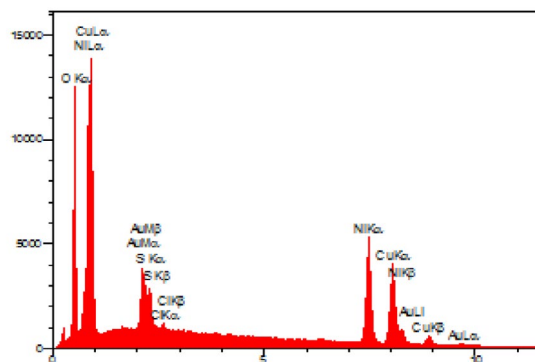


Fig. 2. EDX spectra of B sample (nano-composite containing high Cu content) after calcinations.

plane reflection from the XRD pattern. The EDX spectrum of nano-composite (A) is shown in Fig.2.

Results in Fig. 2 confirm the presence of Ni, O and Cu as the only elementary species in the sample without any other impurity species. The magnetic properties of the synthesized nano-composites were studied with the VSM tool at room temperature. Fig. 3 shows the magnetization curve for prepared nano-structures. The values of the magnetic field [H] and magnetization [M] of the sample were listed in Table 1.

Super paramagnetic properties of the nano composites at magnetic field of -8000 to 8000Oe were confirmed by hysteresis loop of samples shown in the Fig. 3, which means Coercively force (Hc) and Magnetic Remanence (Mr) of nanometer-sized composites are zero or very small. On the other hand, the results in the Fig.3 highlight that the magnetic properties of nano composites are correspond with that of in magnetic materials with sizes greater than 10 nm [22-25]. The hysteresis loop of nanometer-sized composites was attributed to domain structure due to pinning effect of magnetic domain walls at grain boundaries, the magnetic anisotropy of the crystalline lattice as well as impurities within the nano-meter sized structures [22-25, 32]. As can be seen in Fig.3, the saturation magnetization of the magnetic samples

Table 1. The data related to the Optical band gap, Magnetization (M), magnetic field (H), and the average crystallite size of CuO-NiO nano-composites.

sample	Band-gap (ev) after calcination	M (emu/g) before calcination	M (emu/g) after calcination	The average crystallite size (D) of Nano composites	H(Oe) after calcination
A	3.85	0.19536	0.10645	39	150
B	3.99	0.18693	0.07711	34	0

Table 2. In vitro susceptibility testing of 21 clinical vaginal isolates of *C. albicans* (µg/ml).

Antifungal	MFC	MIC50	MIC90	MIC range
Nanoparticles	7.81	1.95	3.90	0.97-15.62
Fluconazole	12.5	3.12	6.25	1.75-25

is depends on the Cu content in nano composite, as well as less than that of the Nio bulk materials (55 emu/g) [22-26].

It is clear from data in Table 2 that the magnetization (M) and coercively force (Hc) of CuO-NiO nano materials decreased with the reduction in the size of nano-composite. This magnetic behavior of nano materials can be assigned the competition between the F-centre exchange coupling (FCE) coupling and super-exchange coupling in the nano composite with a change in their size due to variation in the structure of the domain, size and surface effect in nanoscale-sized structures [24, 32-33]. The SEM image of synthesized nanometer-sized particles is shown in Fig.4. It can be seen in Fig.4 that the synthesized nano-composites are to form of shape-like aggregated nano-clusters due to van der Waals force between particles [22-25]. The observed average size of sample (A) from SEM images was about 30nm. Hydrodynamic size of B sample in cell culture medium is shown in Fig.5. The UV-Vis spectra of CuO-NiO nano composites after calcinations are shown in Fig.7 that was measured using a USB-2000 UV-Vis spectrophotometer.

Fig.7 shows that the absorption edge of nano-composites there is in the range of 200-350 nm. The blue shift of absorption edge for nanometer-sized samples was attributed to decrease in size of particles due to increase in Cu content in the composite based

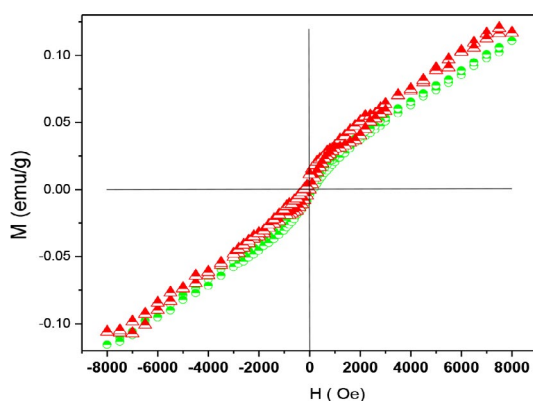


Fig. 3. M-H curves of CuO- NiO Nano composite (up triangle): A sample and (circle): B sample after calcination.

on the quantum size effect of nano structures.

The obtained direct optical band gap values for samples are shown in Fig.8. It is necessary to mention that the optical direct band gap values of the samples were determined by Tauc's relation [21-22]:

$$\alpha h\nu = \alpha_0 (h\nu - E_g)^{1/2} \quad (1)$$

Where $h\nu$, α_0 and E_g are photon energy, a constant and optical band gap of the nanoparticles, respectively. Absorption coefficient (α) of the samples can be calculated from the absorption spectra at different wavelengths. The values of E_g were determined by extrapolations of the linear regions of the plot of versus .

As seen in Fig. 8, value of optical band gap increases with increase Cu content in the system.

Cytotoxic evaluation

The result of the cytotoxic study of nano-composites on MDA cells of Breast cancer is shown in Fig.9. From Fig.9 it can be seen that nano-composites demonstrate no significant toxicity at the lower concentrations. However, mean cell viability at a concentration of 50µg/ml and 10µg/ml was equivalent to %60 and %80, respectively.

In the current research, three wells of 96-well culture plates were the mixture of nanoparticles and MTT reagent without cells, which were used as blanks and for evaluating of different dilution of

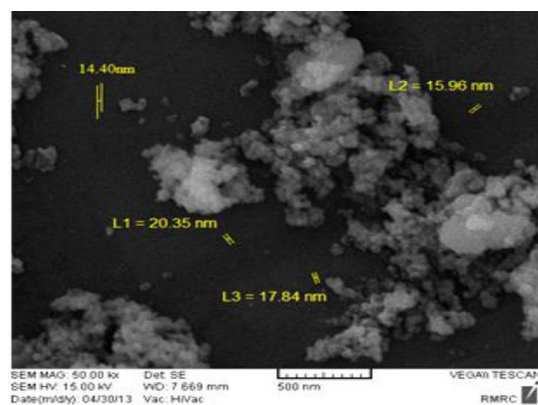


Fig. 4. SEM image of a sample (nano composite containing low Cu content)after calcinations.

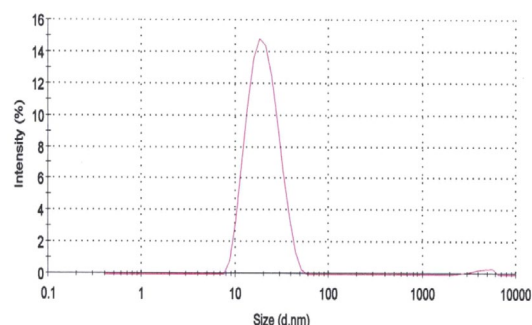


Fig. 5. Hydrodynamic size of B sample (nano-composite containing high Cu content) in cell culture medium

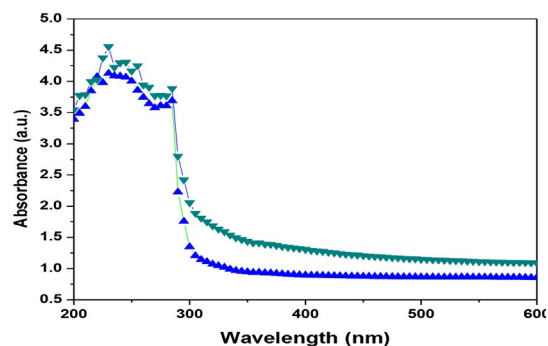


Fig. 7. UV- Vis spectra of CuO-NiO nano-composites after calcinations.

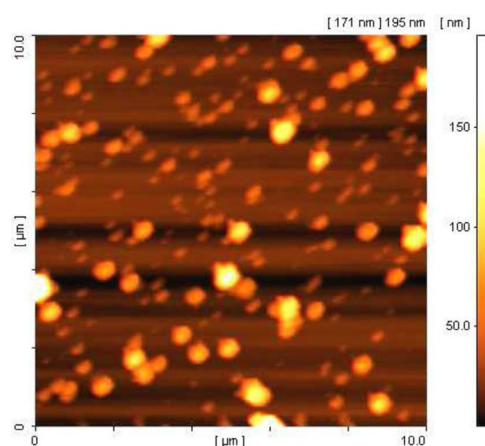


Fig.6. AFM image of sample with B sample (nano-composite containing high Cu content) before calcinations.

nanoparticle was added cell suspension from the petri dish into each well of the required 96-well culture plates. In comparison, Moses et al (2015) based on their study about Cytotoxicity effects of nanoparticles (AuNPs) on MCF-7 and MDA-MB-231 Breast Cancer Cells reported that MDA-MB-231 cells greater sensitivity to the mixture than the MCF-7 cells, particularly using the extra strength mixture ($IC_{50} = 0.013\%$ vs. 0.04%) [33]. Similarly, Suganya et al (2016) assessed the cytotoxic effect of synthesized AuNPs on MDA-MB-231 cells using MTT assay and They not observed 50% inhibition in cell proliferation in the cell lines for all the dosages after 24 h incubation [39]. In another paper, Abbasali pourkabir et al found that cytotoxicity effects of solid lipid nanoparticle (SLN) on MDA-MB231 cell lines were low [40]. In another study, the cytotoxicity assay by MTT method for Nanobiocide has been performed [41]. So, although there were several studies about non-cytotoxicity effects of other nanoparticles including

AuNPs on MDA-MB cells; however, there is no published report about the CuO- NiO nano-composites effects on MDA-MB cells.

In vitro Minimum inhibitory concentration (MIC)

Table 2 includes the study result of MIC of Fluconazole and nano-composites (B sample) against vaginal isolates of *C. albicans*. The data in Table 2 clearly demonstrates that the nano-composites have potent antifungal activity against vaginal isolates of *C. albicans* in comparison with Fluconazole. It is important to mention that Ghahremanloo et al conducted a study based on the antifungal activity of the silver nanoparticles with different concentration against *Candida albicans*. They reported that the highest mean difference for standard *Candida albicans* for 2.5% concentration of nanoparticles after 24 hours of exposure time was 501.0 ± 23.1 , whereas for concentrations of 5% and 10% of nano-meter sized particles after 6 hours of exposure time was

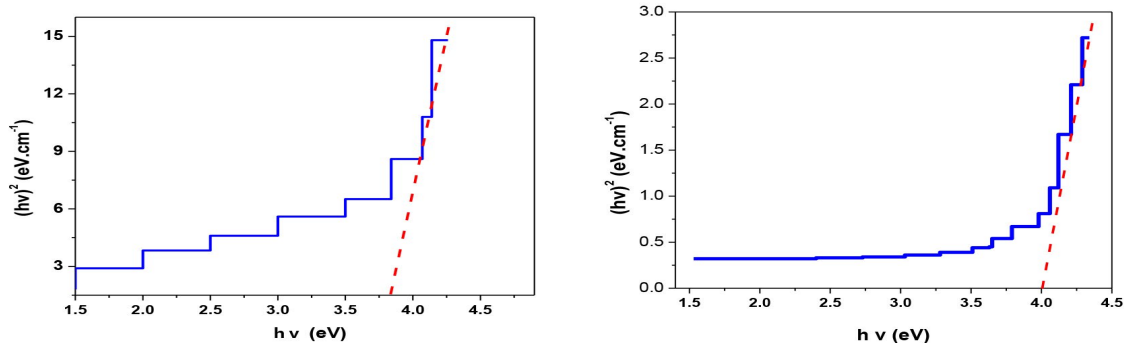


Fig.8. The $(ah\nu)^2$ as a function of $h\nu$ spectra of (right): A sample and (left): A sample

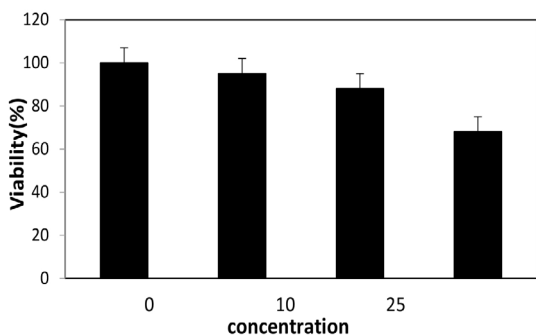


Fig.9. Cytotoxic effects of different concentrations of B sample on MDA cells of Breast cancer.

953±87, 1000±24.9, respectively [34]. In another study by Alipoor et al, Minimum inhibitory and fungicidal concentrations of gold nanoparticle were determined 6.25, 12.5 ppm and for Fluconazole were 50.25±19.48 and 100.50±38.96, respectively, and they reported that antifungal activity of gold nanoparticle was dependent on concentration [35].

CONCLUSIONS

The CuO-NiO nano-composites synthesized by precipitation method in the absence of capping agent. The absorption peak of nanoparticles appears at around 200-350 nm. The reduction in size and increase in the band gap of nanoparticle was observed with increase in Cu content in nano-composite. The XRD pattern analysis of CuO-NiO nano-composites showed that the synthesized samples are in a cubical phase. The average size of samples was found about 20-40nm as calculated by XRD and SEM techniques. Spherical-like morphology of nano composites was confirmed by the AFM and SEM images. Magnetization characterization of CuO-NiO nano-composite by using VSM technique indicated a decrease in their magnetic property with the increase in Cu content in the system.

Antifungal study of CuO-NiO nano-composites on against vaginal isolates of *C.lbicans* indicated an MIC90 antifungal activity with 3.90µg/ml. Results of cytotoxicity study of nano- composites at the lower concentrations on Breast cancer MDA cell lines demonstrate no significant toxicity.

ACKNOWLEDGEMENT

The authors are grateful to the University of Sistan and Baluchestan for financial support.

CONFLICT OF INTEREST

The authors declare that there are no conflicts of interest regarding the publication of this manuscript.

REFERENCES

1. Singh N, Manshian B, Jenkins GJ, Griffiths SM, Williams PM, Maffei TG, Wright CJ, Doak SH. NanoGenotoxicology: the DNA damaging potential of engineered nanomaterials. *Biomaterials*. 2009;30:3891-914.
2. Pei L, Zhang X, Zhang L, Zhang Y, Xu Y. Solvent influence on the morphology and supercapacitor performance of the nickel oxide. *Mater. Lett*. 2016;162:238-41.
3. Mahato TH, Singh B, Srivastava AK, Prasad GK, Srivastava AR, Ganesan K, Vijayaraghavan R. Effect of calcinations temperature of CuO nanoparticle on the kinetics of decontamination and decontamination products of sulphur mustard. *J. Hazard. Mater*. 2011;192:1890-5.
4. Gajendiran J, Rajendran V. Synthesis and characterization of coupled semiconductor metal oxide (ZnO/CuO) nanocomposite. *Mater. Lett*. 2014;116:311-3.
5. Gajendiran J, Ramamoorthy C, Sankar KP, Kingsly TR, Kamalakannan V, Krishnamoorthy T. Optical and Luminescent Properties of NiO-CuO Nanocomposite by The Precipitation Method. *J.Advanc Chem Sci*, 2016;227-9.
6. Solanki PR, Kaushik A, Agrawal VV, Malhotra BD.

- Nanostructured metal oxide-based biosensors. *NPG Asia Mater.* 2011;3:17-24.
7. Ghanbari K, Babaei Z. Fabrication and characterization of non-enzymatic glucose sensor based on ternary NiO/CuO/polyaniline nanocomposite. *Anal. Biochem.* 2016;498:37-46.
 8. Hassanpour M, Safardoust H, Ghanbari D, Salavati-Niasari M. Microwave synthesis of CuO/NiO magnetic nanocomposites and its application in photo-degradation of methyl orange. *J. Mater. Sci-Mater. El.* 2016;27:2718-27.
 9. Said AE, El-Wahab MM, Soliman SA, Goda MN. Synthesis and Characterization of Nano CuO-NiO Mixed Oxides. *Nanosci. Nanotechnol.* 2014;2:17-28.
 10. Lenggoro IW, Itoh Y, Iida N, Okuyama K. Control of size and morphology in NiO particles prepared by a low-pressure spray pyrolysis. *Mater Res. Bull.* 2003;38:1819-27.
 11. Ma CL, Sun XD. Preparation of nanocrystalline metal oxide powders with the surfactant-mediated method. *Inorg Chem. Commun.* 2002;5:751-5.
 12. Wang CB, Gau GY, Gau SJ, Tang CW, Bi JL. Preparation and characterization of nanosized nickel oxide. *Catal. Lett.* 2005;101:241-7.
 13. Tao D, Wei F. New procedure towards size-homogeneous and well-dispersed nickel oxide nanoparticles of 30 nm. *Mater. Lett.* 2004;58:3226-8.
 14. Wang Y, Ke JJ. Preparation of nickel oxide powder by decomposition of basic nickel carbonate in microwave field with nickel oxide seed as a microwave absorbing additive. *Mater. Res. Bull.* 1996;31:55-61.
 15. Illy-Cherrey S, Tillement O, Dubois JM, Massicot F, Fort Y, Ghanbaja J, Bégin-Colin S. Synthesis and characterization of nano-sized nickel (II), copper (I) and zinc (II) oxide nanoparticles. *Mater. Sci Eng.A.* 2002;338:70-5.
 16. Li C, Zhang D, Liu X, Han S, Tang T, Han J, Zhou C. Chemical capping synthesis of nickel oxide nanoparticles and their characterizations studies. *Appl Phys Lett.* 2003;82: 1613.
 17. Theivasanthi T, Venkadamani G, Palanivelu M, Alagar M. Nano sized Powder of Jackfruit Seed: Spectroscopic and Anti-microbial Investigative Approach. *Nano Biomed Eng.* 2011;3:1-6.
 18. Rahdar A, Aliahmad M, Asnaashari H. Effect of Different Capping Agents on the Undoped ZnS Semiconductor Nanocrystals: Synthesis and Optical and Structural Characterization. *Adv. Sci. Lett.* 2013;19:547-9.
 19. Rahdar A, Aliahmad M, Azizi Y. NiO Nanoparticles: Synthesis and Characterization. *J. Nanostruct.* 2015;5:145-51.
 20. Pankhurst QA, Connolly J, Jones SK, Dobson JJ. Applications of magnetic nanoparticles in biomedicine. *J. Phys. D: Appl. Phys.* 2003;36:R167.
 21. Tauc J. *Optical Properties of Solids*, New York: Academic Press Inc;1966.
 22. Rahdar A, Aliahmad M, Azizi Y. Synthesis of Cu Doped NiO Nanoparticles by Chemical Method. *J Nanostruct.* 2014;4:145-52.
 23. Hartley PA, Parfitt GD, Pollack LB. The role of the van der Waals force in the agglomeration of powders containing submicron particles. *Power Tech.* 1985;42:35-46.
 24. Kumar S, Kim YJ, Koo BH, Lee CG. Structural and magnetic properties of Ni doped CeO₂ nanoparticles. *J Nanosci Nanotechnol.* 2010;10:7204-7.
 25. Aliahmad M, Rahdar A, Sadeghfard F, Bagheri S, Hajinezhad MR. Synthesis and Biochemical effects of magnetite nanoparticle by surfactant-free electrochemical method in an aqueous system: The current density effect. *Nanomed Res J.* 2016;1:39-46.
 26. Hwang JH, Dravid VP, Teng MH, Host JJ, Elliott BR, Johnson DL, Mason TO. Magnetic properties of graphitically encapsulated nickel nanocrystals. *J. Mater. Res.* 1997;12:1076-82.
 27. Stockert JC, Blázquez-Castro A, Cañete M, Horobin RW, Villanueva Á. MTT assay for cell viability: Intracellular localization of the formazan product is in lipid droplets. *Acta histochemica.* 2012;114:785-96.
 28. Marshall NJ, Goodwin CJ, Holt SJ. A critical assessment of the use of microculture tetrazolium assays to measure cell growth and function. *Growth Regul.* 1995;5:69-84.
 29. Mosmann T. Rapid colorimetric assay for cellular growth and survival: application to proliferation and cytotoxicity assays. *J Immunol Methods.* 1983;65:55-63.
 30. Pfaller MA, Chaturvedi V, Espinel-Ingroff A, Ghannoum MA, Gosey LL, Odds FC, Rex JH, Rinaldi MG, Sheehan DJ, Walsh TJ, Warnock DW. National Committee for Clinical Laboratory Standards, reference method for broth dilution antifungal susceptibility testing of yeasts. NCCLS Document M27eMA2 NCCLS. Pennsylvania, USA. 2002.
 31. Saadat E, Amini M, Dinarvand R, Dorkoosh FA. Polymeric micelles based on hyaluronic acid and phospholipids: Design, characterization, and cytotoxicity. *Inc. J. Appl. Polym. Sci.* 2014;131.
 32. Khoshnevisan K, Barkhi M, Ghasemzadeh A, Tahami HV, Pourmand S. Fabrication of Coated/Uncoated Magnetic Nanoparticles to Determine Their Surface Properties. *Mater. Manuf. Process.* 2016;31:1206-15.
 33. Moses SL, Edwards VM, Brantley E. Cytotoxicity in MCF-7 and MDA-MB-231 Breast Cancer Cells, without Harming MCF-10A Healthy Cells. *J Nanomed Nanotechnol.* 2016;7: 2.
 34. Ghahremanloo A, Rajabi O, Ghazvini K, Mirmortazavi A, MOTEVALI HM. Antifungal effect of silver nanoparticles in acrylic resins. Antifungal Effect of Silver Nanoparticles in Acrylic Resins. *J Mash Dent Sch.* 2013; 37:239-248.

35. Alipoor J, Madani M, Naghsh N, Bayat M. Investigation of the Effect of Gold Nanoparticles on Vital Factors of Isolated *Candida albicans* in Patients with Vulvovaginal Candidiasis In Vitro. *J. Ardabil Univ. Med. Sci.* 2015;15:179-88.
36. Mahmoodi NM, Hosseinabadi-Farahani Z, Bagherpour F, Khoshrou MR, Chamani H, Forouzesfar F. Synthesis of CuO–NiO nanocomposite and dye adsorption modeling using artificial neural network. *Desalin. Water Treat.* 2016;57:17220-9.
37. Devadathan D, Raveendran R. Polyindole based nickel-zinc oxide nanocomposite-characterization and antifungal studies. *Int J Chem Eng Appl.* 2014;5:240.
38. Aljani Z, Talebian N, Doudi M. Bactericidal Activity of Copper Oxide Nanocomposite/Bioglass for in Vitro Clindamycin Release in Implant Infections Due to *Staphylococcus aureus*. *Avicenna j. med. biochem.* 2016;4:1-10.
39. KS US, Govindaraju K, Kumar G, Prabhu D, Arulvasu C, Karthick V, Changmai N. Anti-proliferative effect of biogenic gold nanoparticles against breast cancer cell lines (MDA-MB-231 & MCF-7). *Appl. Surf. Sci.* 2016;371:415-24.
40. Abbasalipourkabirreh R, Salehzadeh A, Abdullah R. Cytotoxicity effect of solid lipid nanoparticle on human breast cancer cell lines. *Biotechnology.* 2011;10:528-33.
41. Hemmati M, Ghasemzadeh A, Haji Malek-kheili M, Khoshnevisan K, Koochi MK. Investigation of acute dermal irritation/corrosion, acute inhalation toxicity and cytotoxicity tests for Nanobiocide®. *Nanomed Res J.* 2016;1:23-9.